

Hydration state inside HeLa cell monolayer investigated with terahertz spectroscopy

K. Shiraga, T. Suzuki, N. Kondo, K. Tanaka, and Y. Ogawa

Citation: [Applied Physics Letters](#) **106**, 253701 (2015); doi: 10.1063/1.4922918

View online: <http://dx.doi.org/10.1063/1.4922918>

View Table of Contents: <http://scitation.aip.org/content/aip/journal/apl/106/25?ver=pdfcov>

Published by the [AIP Publishing](#)

Articles you may be interested in

[Hydration and hydrogen bond network of water around hydrophobic surface investigated by terahertz spectroscopy](#)

J. Chem. Phys. **141**, 235103 (2014); 10.1063/1.4903544

[Observation of salt effects on hydration water of lysozyme in aqueous solution using terahertz time-domain spectroscopy](#)

Appl. Phys. Lett. **103**, 173704 (2013); 10.1063/1.4826699

[Determination of the complex dielectric constant of an epithelial cell monolayer in the terahertz region](#)

Appl. Phys. Lett. **102**, 053702 (2013); 10.1063/1.4790392

[Real-time sonoporation through HeLa cells](#)

AIP Conf. Proc. **1474**, 271 (2012); 10.1063/1.4749348

[Label-free monitoring of interaction between DNA and oxaliplatin in aqueous solution by terahertz spectroscopy](#)

Appl. Phys. Lett. **101**, 033704 (2012); 10.1063/1.4737401



MMR TECHNOLOGIES

**THE WORLD'S RESOURCE FOR
VARIABLE TEMPERATURE
SOLID STATE CHARACTERIZATION**

WWW.MMR-TECH.COM

OPTICAL STUDIES SYSTEMS SEEBECK STUDIES SYSTEMS MICROPROBE STATIONS HALL EFFECT STUDY SYSTEMS AND MAGNETS

Hydration state inside HeLa cell monolayer investigated with terahertz spectroscopy

K. Shiraga,¹ T. Suzuki,¹ N. Kondo,¹ K. Tanaka,² and Y. Ogawa^{1,a)}

¹Graduate School of Agriculture, Kyoto University, Kyoto 606-8502, Japan

²Department of Physics, Kyoto University, Kyoto 606-8502, Japan

(Received 13 March 2015; accepted 11 June 2015; published online 23 June 2015)

The hydration state in living cells is believed to be associated with various cellular activities. Nevertheless, *in vivo* characterization of intracellular hydration state under physiological condition has not been well documented to date. In this study, the hydration state of an intact HeLa cell monolayer was investigated by terahertz time-domain attenuated total reflection spectroscopy. Combined with the extended theory of Onsager, we found $23.8 \pm 7.4\%$ of HeLa intracellular water was hydrated to biomolecules (corresponding to 1.25 g H₂O/g solute); exhibiting slower relaxation dynamics than bulk water. © 2015 AIP Publishing LLC. [<http://dx.doi.org/10.1063/1.4922918>]

Liquid water, sometimes referred to as the “matrix of life,” orchestrates the expression of biological macromolecules, which determines the functional and metabolic state of living cells. In particular, small changes in protein conformation can be associated with cascading effects on the surrounding water molecules: if the conformational change ties up more hydration water (dynamically retarded water in the vicinity of biomolecules), the protein structure becomes more rigid and, at the same time, the diffusion in the surrounding medium is retarded, conversely, if more bulk water is released, the conformation becomes more mobile and the fluidity of the surrounding medium increases.¹ Simultaneously, the hydration state of the intracellular biomolecules themselves influences the surrounding chemical interactions as well as their own conformational stability, because the net rate of metabolic processes within the cell depends on the diffusion rate of molecules.² In turn, we can assume that the intracellular hydration state will influence, to a degree, the activity of the cell itself. In fact, it has been proposed that “osmotically unresponsive and viscous” hydration water predominates in a resting cell, however, when “reactive and fluid” bulk water becomes more abundant, the cell will switch to an active one.^{3,4} This hypothesis seems to be consistent with previous nuclear magnetic resonance (NMR) results that suggest water in cancerous (= active) tissues is characterized by increased fluidity compared to that in normal (= stable) tissues,⁵ indicating that cellular activity and pathological states are closely associated with intracellular hydration states.

Spectroscopic methods, such as NMR,⁶ quasi-elastic neutron scattering (QENS),^{7,8} and incoherent neutron scattering (INS)^{9–11} have been used in the last decade to quantitatively determine the hydration state of monocellular organisms (i.e., *Escherichia coli* and *Haloarcula marismortui*) and human red blood cells. These studies show that 85%–90% of intracellular water behaves in a bulk-like fashion, while the remaining water molecules (classified as hydration water) exhibit more retarded reorientation and translation dynamics than that of bulk water. However, since

the organelles and chemical composition of these cells are substantially different from those of general eukaryotic cells, the present understanding of intracellular hydration cannot be said to have reached a consensus. Furthermore, current *in vivo* estimation of hydration state is impeded by two issues: first, these techniques cannot spatially distinguish between intracellular and extracellular water. Consequently, any extracellular water within the sampling window will be included in the measurement and obscure, to a degree, the measurement of the “true” intracellular hydration state. Second, hydrogen/deuterium (H/D) substitution or cryogenic cooling is needed in these methods, thus, the “native” hydration state in the cell interior is not directly measured. To overcome these difficulties, nonlinear optical Kerr effect (OKE) microspectroscopy, which probes only a spatially confined volume (0.5 μm in the lateral direction and 4.0 μm in the axial coordination) inside a single living cell, has been employed without the need for H/D substitution or cryogenic cooling of the target mammalian culture cell.¹² As a result, it was shown that the water inside an intact mammalian culture cell under physiological conditions exhibited a 1.7 times slower structural relaxation than that of pure water. This data indicates the mobility of intracellular water is, on average, moderately restricted due to the presence of biological macromolecules and hydration water. However, as far as intracellular water is concerned, firm conclusions cannot yet be drawn due to insufficient experimental evidence.¹³

Recently, terahertz (THz) spectroscopy has attracted attention as a method for determining hydration state.^{14–17} Dielectric responses to the THz waves, whose periodic electric field corresponds to the lifetime of bulk water hydrogen bonds,¹⁸ are dominated by relaxational dynamics of bulk water molecules. On the other hand, the relaxation motion of hydration water, which lies below the GHz frequencies, has negligible contribution in the THz region.¹⁴ Accordingly, the dielectric responses in the THz region are selectively sensitive to bulk water, consequently, any decreases in the THz signal one can use to evaluate the hydration state of cells without the need for any preprocessing such as H/D substitution. Additionally, the long wavelength and low photon energy of THz waves (300 μm and 4 meV at 1 THz,

^{a)}Author to whom correspondence should be addressed. Electronic mail: ogawayu@kais.kyoto-u.ac.jp

respectively), relative to those in the optical frequency region, allow one to observe whole living cells (typical cell size: several tens μm in the planar diameter and several μm in the thickness) under physiological conditions.^{19,20} In this study, therefore, we characterized the spatially averaged hydration state inside living culture cells (HeLa, human cervical carcinoma); a measurement based on the complex dielectric constant in the THz region of the *in vivo* HeLa cell monolayer.

In order to determine the complex dielectric constant of the cultured HeLa cells, THz time-domain attenuated total reflection spectroscopy (THz TD-ATR) was employed.²¹ The ATR geometry allows one to accurately measure the complex dielectric constants of samples with strong absorption in the THz region, such as water-rich living cells, compared to transmission or external reflection geometries.²² The HeLa cells were cultured, in a minimum essential medium (MEM), on a silicon ATR prism of a THz TD-ATR spectrometer, TAS7500 (ADVANTEST Co., Ltd.). The cell incubation chamber was set up on top of the ATR prism, and maintained at 310 K and supplied with a humidified 5% CO_2 atmosphere. The growth of the cultured cells was observed through the transparent lid of the incubation chamber with an optical microscope. After confirming that the HeLa culture cells had formed a monolayer on the ATR prism, the THz TD-ATR measurements were performed over the range of 0.25 and 3.5 THz. More than 4.0×10^4 scans were carried out within 75 min, and to confirm the repeatability, four different samples were measured on different days and then averaged. In our measurements, the standard errors in the real and imaginary part of the complex dielectric constant were at most 0.020 and 0.025 below 1.0 THz, and 0.090 and 0.045 between 1.0 and 3.5 THz, respectively.

The observed complex dielectric constant of HeLa cells in the MEM is compared with that of distilled water and the MEM in Figure 1. We found the dielectric responses of the MEM were unchanged from those of distilled water, but HeLa cells in the MEM can be distinguished from the MEM. In our THz TD-ATR setup, the localization depth of the evanescent field (estimated to be 23 μm at 1.0 THz when the sample is water²³) is greater than the thickness of the HeLa cell monolayer ($7.5 \pm 1.0 \mu\text{m}$ ²⁰). Therefore, the complex dielectric constant of HeLa cells in the MEM in Figure 1 reflected both the dielectric responses of HeLa cells (directly adhered to the ATR prism) and the MEM (on the top of HeLa cells). To determine the complex dielectric constant of the HeLa cell monolayer alone, removing the contribution of the MEM above the HeLa cells, a two-interface model consisting of the ATR prism—HeLa monolayer and HeLa—medium boundaries (see the schematic illustration in the inset of Figure 1). In this calculation, the non-uniformity ($\pm 1.0 \mu\text{m}$) in the HeLa cell monolayer interface was taken into account by assuming that the cell monolayer is flat $7.5 \pm 1.0 \mu\text{m}$. Since the (complex) dielectric constants of the ATR prism and the MEM as well as the incident angle and the thickness of the cell monolayer are known, the complex dielectric constant of the HeLa cell monolayer can be calculated theoretically. Details of the calculation process are presented in earlier papers.^{19,20}

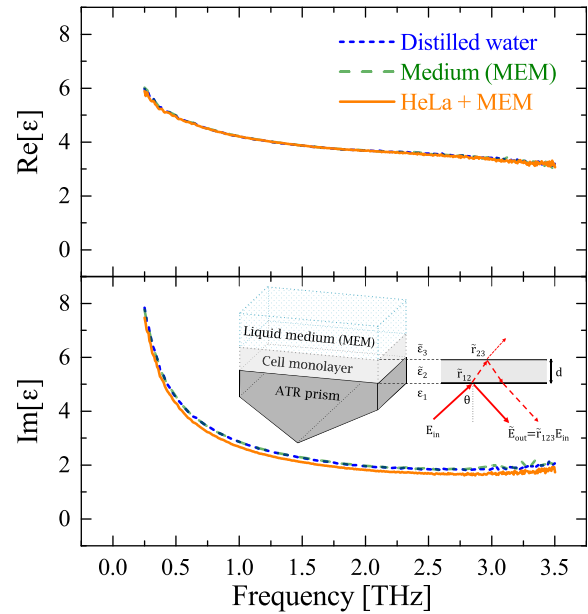


FIG. 1. Complex dielectric constant of distilled water, MEM, and HeLa cells in MEM. The inset shows a schematic illustration of the two-interface model: ϵ_1 , ϵ_2 , ϵ_3 (dielectric constant of the ATR prism, HeLa cell monolayer, and the MEM), \bar{r}_{12} , \bar{r}_{23} (Fresnel's reflection coefficient at each boundary), E_{in} , E_{out} (incident and reflected THz electric field), θ (incident angle), and d (thickness of HeLa cell monolayer).

Figure 2 shows the complex dielectric constants of distilled water, $\tilde{\epsilon}_{\text{water}}(\omega)$, and the HeLa cell monolayer, $\tilde{\epsilon}_{\text{HeLa}}(\omega)$, at 310 K, between 0.25 and 3.5 THz. $\tilde{\epsilon}_{\text{HeLa}}(\omega)$ accords well with the reported extrapolated data of the complex dielectric constant of human tissues measured at 310 K.²⁴ The insets of Figure 2 represent $\delta\tilde{\epsilon}(\omega) = \tilde{\epsilon}_{\text{water}}(\omega) - \tilde{\epsilon}_{\text{HeLa}}(\omega)$, where the error bars in the insets are due to heterogeneity in cellular thickness ($7.5 \pm 1.0 \mu\text{m}$) in the two-interface calculation procedure. As previous studies have suggested, biomolecules dispersed in aqueous solution have

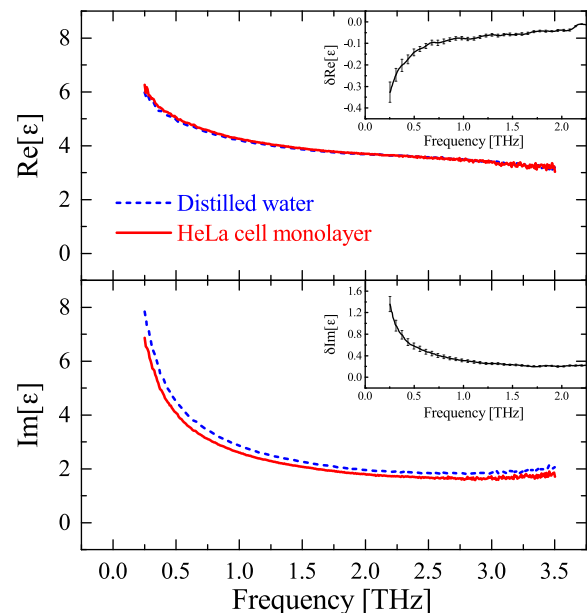


FIG. 2. Comparison of the complex dielectric constants: HeLa cell monolayer $\tilde{\epsilon}_{\text{HeLa}}(\omega)$ and distilled water $\tilde{\epsilon}_{\text{water}}(\omega)$. The insets are the difference in the complex dielectric constants $\delta\tilde{\epsilon}(\omega) = \tilde{\epsilon}_{\text{water}}(\omega) - \tilde{\epsilon}_{\text{HeLa}}(\omega)$.

negligible absorption in the THz region.^{14–16,25} This means that the complex dielectric constants of distilled water and HeLa cell monolayer between 0.25 and 3.5 THz come from Debye-type relaxation and Lorentz-type vibration dynamics of the water molecules and can be expressed as a superposition of the complex susceptibilities of slow relaxation $\tilde{\chi}_{slow}(\omega)$ (collective reorientation of hydrogen-bonded bulk water, ~ 0.02 THz), fast relaxation $\tilde{\chi}_{fast}(\omega)$ (individual reorientation of non-hydrogen-bonded water, ~ 0.5 THz), and intermolecular stretching vibration $\tilde{\chi}_S(\omega)$ (hindered translation of water, ~ 5 THz).²⁶ Among these, the slow relaxation mode of bulk water ($\tau_{slow} \approx 6.33$ ps at 310 K) is distinguishable from that of hydration water. This is because the relaxation time of hydration water molecules is much longer than that of bulk water, thereby the contribution of the hydration water relaxation is negligible above 0.25 THz.¹⁴ In contrast, $\tilde{\chi}_{fast}(\omega)$ and $\tilde{\chi}_S(\omega)$ at sub-picosecond timescales are still present among hydration water molecules since such short-lived water dynamics are less influenced by the hydration effect.

Even though several dielectric functions have been recently demonstrated to describe the terahertz dielectric functions of living objects,^{20,27} it was quite difficult to determine the intracellular hydration state on the basis of these model functions, in principle. Arikawa *et al.* developed a model based on the theory of Onsager, which takes into consideration the local electric field, to determine the hydration parameters for mono-solute aqueous solutions, where water molecules that no longer exhibit the slow relaxation $\tilde{\chi}_{slow}(\omega)$ are defined as hydration water.¹⁴ In this study, aiming to characterize the intracellular hydration state, we extended Arikawa's model to a multi-solute system, where four kinds of biomolecules (protein, lipid, RNA, and DNA) are assumed to be responsible for the hydration state inside the HeLa cell monolayer. In this analysis, $\tilde{\epsilon}_{HeLa}(\omega)$ —determined by experiment—was decomposed into the complex susceptibilities of bulk water $\tilde{\chi}_{bulk}(\omega)$, hydration water $\tilde{\chi}_{hyd}(\omega)$, and biomolecular solutes $\tilde{\chi}_{sol}(\omega)$, via Eq. (1) using a least-square method

$$\begin{aligned} \tilde{\epsilon}_{HeLa}(\omega) - 1 &= \tilde{\chi}_{bulk}(\omega) + \tilde{\chi}_{hyd}(\omega) + \tilde{\chi}_{sol}(\omega) \\ &= \frac{4\pi(N_w - n_h \sum N_s) \tilde{g}(\omega)}{1 - \tilde{\alpha}_{vib}(\omega) \tilde{h}(\omega) / r_w^3} \\ &\quad \times \left\{ \tilde{\alpha}_{vib}(\omega) + \frac{\tilde{\alpha}_{slow}(\omega) + \tilde{\alpha}_{fast}(\omega)}{1 - \alpha_w h / r_w^3} \right\} \\ &\quad + \frac{4\pi n_h \sum N_s \tilde{g}(\omega)}{1 - \tilde{\alpha}_{vib}(\omega) \tilde{h}(\omega) / r_h^3} \\ &\quad \times \left\{ \tilde{\alpha}_{vib}(\omega) + \frac{\tilde{\alpha}_{fast}(\omega)}{1 - \alpha_w h / r_h^3} \right\} \\ &\quad + \sum_{s=p,l,R,D} \frac{4\pi N_s \tilde{g}(\omega)}{1 - \alpha_s \tilde{h}(\omega) / r_s^3} \alpha_s \end{aligned} \quad (1)$$

where, n_h is the number of hydration water molecules per solute molecule, $r_{w(h,s)}$ is the molecular radius of bulk water (hydration water, solute), and $N_{w(s)}$ is the number density of water (solute). $\sum N_s$ is the sum of the number density of proteins (N_p), lipids (N_l), RNA (N_R), and DNA (N_D), $\sum N_s = N_p + N_l + N_R + N_D$ (hereafter, the subscripts of

“p,” “l,” “R,” and “D” represent proteins, lipids, RNA, and DNA, respectively). Here, the frequency-dependent polarizability volumes of slow relaxation $\tilde{\alpha}_{slow}(\omega)$, fast relaxation $\tilde{\alpha}_{fast}(\omega)$, and vibration $\tilde{\alpha}_{vib}(\omega)$ were calculated from $\tilde{\chi}_{slow}(\omega)$, $\tilde{\chi}_{fast}(\omega)$, and $\tilde{\chi}_S(\omega)$ that were noted in our previous paper.²⁰ Polarizability volume of the solute (α_s) was assumed to be a frequency-independent real number because there is no frequency dispersion of solutes in aqueous solution.¹⁴ $\tilde{g}(\omega) = 3\tilde{\epsilon}_{HeLa}(\omega) / \{2\tilde{\epsilon}_{HeLa}(\omega) + 1\}$ and $\tilde{h}(\omega) = 2\{\tilde{\epsilon}_{HeLa}(\omega) - 1\} / \{2\tilde{\epsilon}_{HeLa}(\omega) + 1\}$ are the local correlation terms for the external electric field and reaction electric field, respectively. α_w is the high frequency limit ($\omega \rightarrow \infty$) of $\tilde{\alpha}_{vib}(\omega)$, while h is the zero frequency limit ($\omega \rightarrow 0$) of $\tilde{h}(\omega)$. Furthermore, the volume conservation law

$$\frac{4\pi r_w^3}{3} (N_w - n_h \sum N_s) + \frac{4\pi r_h^3}{3} n_h \sum N_s + \sum \frac{4\pi r_s^3}{3} N_s = 1 \quad (2)$$

is simultaneously solved with Eq. (1). For a successful fit, the molecular radius of the solutes (r_s) was fixed (assumed to be spherical in shape), which can be calculated by

$$r_s = \sqrt[3]{\frac{3M}{4\pi N_A \rho}}, \quad (3)$$

where M is the molecular weight, N_A is the Avogadro number, and ρ is the density. At the same time, the polarizability volume of the solutes (α_s) was theoretically calculated from the high-frequency dielectric constant of pure solutes via the Clausius–Mossotti equation,²⁸ and treated as fixed values. Furthermore, to increase the number of fixed parameters, the number densities of solute molecules were expressed as a function of N_w , based on the fraction of number density ($N_w:N_p:N_l:N_R:N_D$), which was estimated by the mass percent and average molar weight of each component inside HeLa cells. All the cited fixed parameters are listed in Table I. These fixed parameters were substituted into Eqs. (1) and (2) to determine the remaining three fitting parameters (n_h , N_w , and r_h) via a least-square fitting process. Since living cells may have non-negligible individual differences in cellular volume and chemical components, the uncertainty of the best-fitted parameters has to be considered carefully. In this study, $\tilde{\epsilon}_{HeLa}(\omega)$ with errors, originating from both experiment and uncertainty in cellular thickness ($7.5 \pm 1.0 \mu\text{m}$), was substituted in the left-hand side of Eq. (1). Additionally, all molecular radii (r_p , r_l , r_R , and r_D) and polarizability volumes (α_p , α_l , α_R , and α_D) were varied by $\pm 10\%$ in order to consider the uncertainty of the fixed parameters in the right-hand side of Eq. (1).

The resulting decomposition of $\tilde{\epsilon}_{HeLa}(\omega)$ into $\tilde{\chi}_{bulk}(\omega)$, $\tilde{\chi}_{hyd}(\omega)$, and $\tilde{\chi}_{sol}(\omega)$ is shown in Figure 3, together with the fitted parameters (n_h , N_w , and r_h). Figure 3 clearly indicates that the complex dielectric constant of the HeLa cell monolayer was fitted with the fitted parameters $n_h = 293.6 \pm 19.6$, $N_w = 0.0312 \pm 0.002/\text{\AA}^3$, and $r_h = 1.78 \pm 0.03 \text{\AA}$. Note that $\pm 10\%$ variance in the fixed molecular radii and polarizability volumes did not significantly affect the decomposed

TABLE I. Fixed parameters used in the fitting procedure.

	Water	Protein	Lipid	RNA ^a	DNA
Mass percent (%) ^b	84 (Ref. 29)	11 (Ref. 29)	2.5 (Ref. 30)	0.4 (Refs. 31 and 32)	0.2 (Refs. 31 and 33)
Molecular weight M (g/mol)	18	5.0×10^4 (Ref. 34)	7.0×10^2 (Ref. 35)	2.5×10^6 (Ref. 36)	2.2×10^{12} (Ref. 37)
Normalized mole fraction	1	4.71×10^{-5}	7.65×10^{-4}	3.43×10^{-8}	1.95×10^{-14}
Density $\rho \times 10^{-24}$ (g/Å ³)	0.99	1.37 (Ref. 38)	1.01 (Ref. 39)	1.56 (Ref. 40)	1.70 (Ref. 41)
Molecular radius r_s (Å)	1.9	24.4	6.4	79.8	9.2×10^3
Polarizability α (Å ³)	3.8 (Ref. 14)	5.6×10^3 (Ref. 42)	96 (Ref. 15)	1.2×10^5 (Ref. 42)	1.9×10^{11} (Ref. 42)

^aRibosome RNA, which occupies about 80% among total RNA, was chosen for molecular weight.

^bFor RNA and DNA, mass percent was determined by dividing intracellular RNA³² and DNA³³ mass by HeLa cell mass.³¹

frequency dispersions of $\tilde{\chi}_{bulk}(\omega)$, $\tilde{\chi}_{hyd}(\omega)$, and $\tilde{\chi}_{sol}(\omega)$. Although absorption coefficients of macromolecular powders (i.e., 100% protein powder samples) are around $10\text{--}50\text{ cm}^{-1}$ in the THz region,^{42,43} our rough estimation showed that their absorption coefficient of proteins weighted by their molar-number in the HeLa cells (i.e., molar-number of intracellular protein is estimated to be about 9 times smaller than that of 100% protein powder) was approximately 50–200 times smaller than that of water. Since biomolecular THz absorptions in HeLa cells are expected to have the same order of measurement error, this validates a $\text{Im}[\tilde{\chi}_{sol}(\omega)]$ of approximately 0, as shown in Figure 3.

Based on the number densities ($N_p = 4.7 \times 10^{-5} N_w$, $N_l = 7.7 \times 10^{-4} N_w$, $N_R = 3.4 \times 10^{-8} N_w$, and $N_D = 2.0 \times 10^{-14} N_w$, as shown in Table I) and the best-fitted N_w , the number density of hydration water ($= n_h \sum N_s$) was calculated to be $0.0074 \pm 0.0005/\text{Å}^3$. In this framework, the fraction of hydration water to total intracellular water ($f_{hyd} = n_h \sum N_s / N_w$) was found to be $f_{hyd} = 23.8 \pm 7.4\%$ for intact HeLa cells. This result corresponds to an “average” hydration water amount of 1.25 g H₂O/g solute in HeLa cell monolayer; roughly similar to that of lysozyme (1.4 g H₂O/g protein) and corresponding to three hydration layers.⁴⁴ Additionally, 8% smaller molecular radius of hydration

water, $r_h = 1.78 \text{ Å}$, than that of bulk water (r_w), was consistent with the fact that the dynamical motion of hydration water is slowed down.¹⁴ The relative effective volume of bulk water to hydration water, $(r_w/r_h)^3 \approx 1.27$, suggests a higher density of intracellular hydration water than bulk water by a factor of 27%.

Our estimation of f_{hyd} for intact HeLa cells determined by THz spectroscopy was larger than that of monocellular organisms and human red blood cells (10%–15%) evaluated by NMR⁶ and QENS,⁸ but essentially equivalent to that of cardiac muscle tissue ($\sim 27\%$) estimated by INS.⁹ The relatively smaller f_{hyd} of monocellular organisms⁶ and human red blood cells⁸ may stem from the different chemical components of the cell interior compared to human living cells; these cells are missing some of the organelles found in eukaryotic cells, such as the nuclear envelope and mitochondria, and thus the hydration mechanisms can be thought to be quite different from those in common human cells. Second, even though f_{hyd} of “freshly excised” human cardiac muscle tissue⁹ was similar to that of our study, tissue dissection and enclosure processes before measurement make it difficult to access the “true” *in vivo* intracellular hydration state. Additionally, these measurements require preprocessing such as H/D substitution and cryogenic cooling, which imposes further modification of the intracellular environment. On the other hand, in our measurement, the hydration state of the intact HeLa cell monolayer was experimentally determined under physiological conditions with optimum temperature and pH.

In this study, with the use of THz TD-ATR spectroscopy, combined with the application of the extended theory of Onsager, we determined the hydration state inside an intact HeLa cell monolayer. Our result indicates $23.8 \pm 7.4\%$ of the HeLa intracellular water was bound to biomolecules (i.e., proteins, lipid, RNA, and DNA), which corresponds to 1.25 g H₂O/g solute of hydration water. These intracellular hydration water molecules exhibited slowed down reorientation dynamics relative to that of bulk water. This *in vivo* characterization of intracellular hydration state under physiological conditions opens up the possibilities of further delving into the anomalous properties of cell water⁴⁵ and offers various potential applications in clinical diagnosis and tissue engineering in the future.

We are grateful to Mr. Motoki Imamura and Mr. Akiyoshi Irisawa (ADVANTEST Corporation, Japan) for their technical supports. We also acknowledge Associate

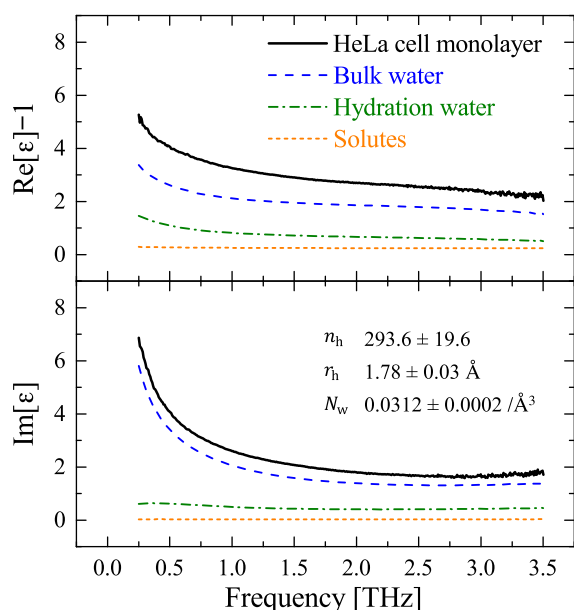


FIG. 3. Decomposition of $\tilde{\chi}_{HeLa}(\omega)$ into the complex susceptibilities of bulk water $\tilde{\chi}_{bulk}(\omega)$, hydration water $\tilde{\chi}_{hyd}(\omega)$, and solutes $\tilde{\chi}_{sol}(\omega)$. The best-fitted parameters are shown in the bottom part.

Professor Garry John Piller (Graduate School of Agriculture, Kyoto University, Japan) for his help and useful discussions. Financial support was provided by Industry-Academia Collaborative R&D from Japan Science and Technology Agency (JST) and JSPS KAKENHI Grant No. 26295.

- ¹M. Chaplin, *Nat. Rev. Mol. Cell. Biol.* **7**, 861 (2006).
- ²P. B. Weisz, *Science* **179**, 433 (1973).
- ³P. M. Wiggins, *Cell Biol. Int.* **20**, 429 (1996).
- ⁴G. D. Fullerton, K. M. Kanal, and I. L. Cameron, *Cell Biol. Int.* **30**, 86 (2006).
- ⁵R. Damadian, *Science* **171**, 1151 (1971).
- ⁶E. Persson and B. Halle, *Proc. Natl. Acad. Sci. U.S.A.* **105**, 6266 (2008).
- ⁷M. Tehei, B. Franzetti, K. Wood, F. Gabel, E. Fabiani, M. Jasnin, M. Zamponi, D. Oesterhelt, G. Zaccai, M. Ginzburg, and B.-Z. Ginzburg, *Proc. Natl. Acad. Sci. U.S.A.* **104**, 766 (2007).
- ⁸A. M. Stadler, J. P. Embs, I. Digel, G. M. Artmann, T. Unruh, G. Büldt, and G. Zaccai, *J. Am. Chem. Soc.* **130**, 16852 (2008).
- ⁹R. C. Ford, S. V. Ruffle, A. J. Ramirez-Cuesta, I. Michalarias, I. Beta, A. Miller, and J. Li, *J. Am. Chem. Soc.* **126**, 4682 (2004).
- ¹⁰M. Jasnin, A. Stadler, M. Tehei, and G. Zaccai, *Phys. Chem. Chem. Phys.* **12**, 10154 (2010).
- ¹¹F. Sebastiani, A. Orecchini, A. Paciaroni, M. Jasnin, G. Zaccai, M. Moulin, M. Haertlein, A. De Francesco, C. Petrillo, and F. Sacchetti, *Chem. Phys.* **424**, 84 (2013).
- ¹²E. O. Potma, W. P. de Boeij, and D. A. Wiersma, *Biophys. J.* **80**, 3019 (2001).
- ¹³P. Ball, *Chem. Phys. Chem.* **9**, 2677 (2008).
- ¹⁴T. Arikawa, M. Nagai, and K. Tanaka, *Chem. Phys. Lett.* **457**, 12 (2008).
- ¹⁵M. Hishida and K. Tanaka, *Phys. Rev. Lett.* **106**, 158102 (2011).
- ¹⁶K. Shiraga, T. Suzuki, N. Kondo, and Y. Ogawa, *J. Chem. Phys.* **141**, 235103 (2014).
- ¹⁷K. Shiraga, H. Naito, T. Suzuki, N. Kondo, and Y. Ogawa, *J. Phys. Chem. B* **119**, 5576 (2015).
- ¹⁸B. Bagchi, *Chem. Rev.* **105**, 3197 (2005).
- ¹⁹K. Shiraga, Y. Ogawa, T. Suzuki, N. Kondo, A. Irisawa, and M. Imamura, *Appl. Phys. Lett.* **102**, 053702 (2013).
- ²⁰K. Shiraga, Y. Ogawa, T. Suzuki, N. Kondo, A. Irisawa, and M. Imamura, *J. Infrared Millimeter, Terahertz Waves* **35**, 493 (2014).
- ²¹M. Nagai, H. Yada, T. Arikawa, and K. Tanaka, *Int. J. Infrared Millimeter Waves* **27**, 505 (2006).
- ²²P. U. Jepsen, D. G. Cooke, and M. Koch, *Laser Photonics Rev.* **5**, 124 (2011).
- ²³K. Ohta and R. Iwamoto, *Appl. Spectrosc.* **39**, 418 (1985).
- ²⁴S. Gabriel, R. W. Lau, and C. Gabriel, *Phys. Med. Biol.* **41**, 2271 (1996).
- ²⁵B. Born and M. Havenith, *J. Infrared Millimeter, Terahertz Waves* **30**, 1245 (2009).
- ²⁶H. Yada, M. Nagai, and K. Tanaka, *Chem. Phys. Lett.* **473**, 279 (2009).
- ²⁷R. Gente, N. Born, N. Voß, W. Sannemann, J. Léon, M. Koch, and E. Castro-Camus, *J. Infrared Millimeter, Terahertz Waves* **34**, 316 (2013).
- ²⁸T. Arikawa, M. Nagai, and K. Tanaka, *Chem. Phys. Lett.* **477**, 95 (2009).
- ²⁹D. N. Wheatley, M. S. Inglis, M. A. Foster, and J. E. Rimington, *J. Cell Sci.* **88**, 13 (1987).
- ³⁰R. T. Dell'orco and G. Melnykovich, *J. Cell. Physiol.* **76**, 101 (1970).
- ³¹K. Park, J. Jang, D. Irimia, J. Sturgis, J. Lee, J. P. Robinson, M. Toner, and R. Bashir, *Lab Chip* **8**, 1034 (2008).
- ³²J. O. Bishop, J. G. Morton, M. Rosbash, and M. Richardson, *Nature* **250**, 199 (1974).
- ³³G. G. Maul and L. Deaven, *J. Cell Biol.* **73**, 748 (1977).
- ³⁴K. B. Hendil, R. Hartmann-Petersen, and K. Tanaka, *J. Mol. Biol.* **315**, 627 (2002).
- ³⁵B. Alberts, D. Bray, K. Hopkin, A. Johnson, J. Lewis, M. Raff, K. Roberts, and P. Walter, *Essential Cell Biology*, 2nd ed. (Garland Science, 2005).
- ³⁶B. Lewin, *Genes VIII* (Pearson education, Inc., 2004), p. 135.
- ³⁷A. Dobi, M. A. Mahan, and D. V. Agoston, *Electrophoresis* **18**, 12 (1997).
- ³⁸H. P. Erickson, *Biol. Proced. Online* **11**, 32 (2009).
- ³⁹S. M. Johnson and N. Buttress, *Biochim. Biophys. Acta* **307**, 20 (1973).
- ⁴⁰P. Tiollais, F. Galibert, and M. Boiron, *Eur. J. Biochem.* **18**, 35 (1971).
- ⁴¹P. Volpe and T. Eremenko, *Eur. J. Biochem.* **32**, 227 (1973).
- ⁴²A. G. Markelz, A. Roitberg, and E. J. Heilweil, *Chem. Phys. Lett.* **320**, 42 (2000).
- ⁴³C. Zhang, E. Tarhan, A. K. Ramdas, A. M. Weiner, and S. M. Durbin, *J. Phys. Chem. B* **108**, 10077 (2004).
- ⁴⁴G. D. Fullerton, V. A. Ord, and I. L. Cameron, *BBA-Protein Struct. M.* **869**, 230 (1986).
- ⁴⁵K. Luby-Phelps, *Mol. Biol. Cell* **24**, 2593 (2013).